

Cell Reports, Volume 36

Supplemental information

**Actinin BiOLD reveals sarcomere
crosstalk with oxidative metabolism
through interactions with IGF2BP2**

Feria A. Ladha, Ketan Thakar, Anthony M. Pettinato, Nicholas Legere, Shahnaz Ghahremani, Rachel Cohn, Robert Romano, Emily Meredith, Yu-Sheng Chen, and J. Travis Hinson

Figure S1

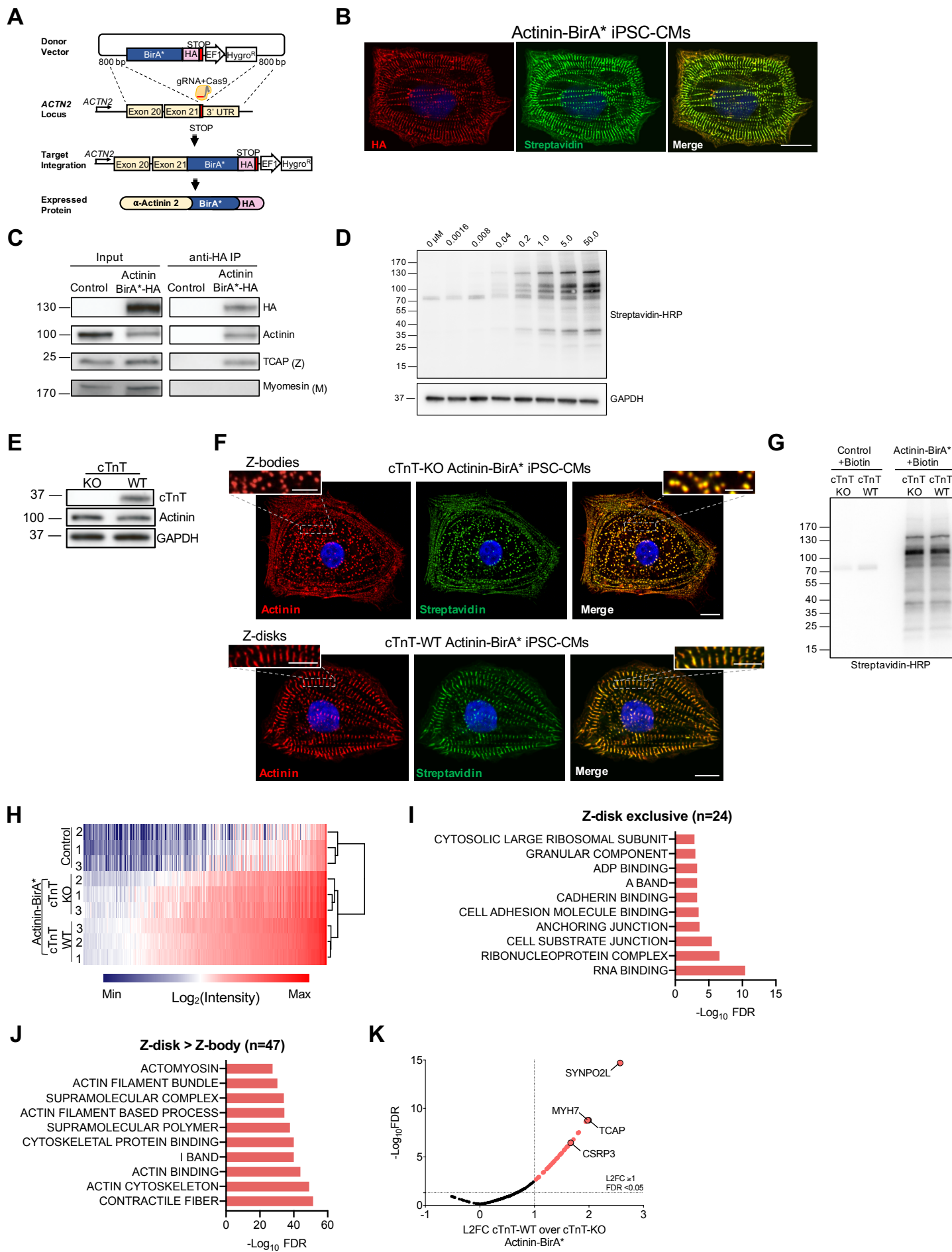


Figure S1. BioID to identify actinin proximity partners through sarcomere assembly. (Related to Figure 1)

(A) Overview of gene-targeting strategy to generate an in-frame knock-in of BirA*-HA at the *ACTN2* locus in iPSCs. CRISPR/Cas9 and homology-directed repair from a donor vector containing BirA*-HA and 800bp *ACTN2* homology arms was utilized.

(B) Confocal micrograph of Actinin-BirA* iPSC-CMs decorated with antibodies to HA (red), streptavidin-AF488 (green), and DAPI DNA co-stain (blue) showing overlap (scale bar=10µm).

(C) To validate localization, iPSC-CM lysates were immunoprecipitated using an anti-HA antibody and probed with antibodies to known sarcomere components at the Z-disk (anti-TCAP) and M-line (anti-myomesin), as well as anti-HA and anti-actinin controls.

(D) Representative immunoblot probed with streptavidin-HRP to optimize biotin labeling after 24 hours of biotin supplementation up to 50 µM.

(E) Representative immunoblot of cTnT-KO and cTnT-WT iPSC-CMs lysates probed for cTnT, actinin and GAPDH control.

(F) Confocal micrograph of cTnT-KO and cTnT-WT Actinin-BirA* iPSC-CMs decorated with antibodies to actinin (red), streptavidin-AF488 (green), and DAPI DNA co-stain (blue) (scale bars: main image=10µm; inset=5µm). In contrast to the Z-disks observed in cTnT-WT iPSC-CMs (bottom), cTnT-KO iPSC-CMs have punctate Z-bodies (top).

(G) Representative immunoblot of cTnT-KO and cTnT-WT Actinin-BirA* lysates probed with streptavidin-HRP.

(H) Significant hits from TMT experiment 2 using hierarchical clustering and heatmap of Log₂-transformed intensity values for the 294 Actinin-BirA*-enriched proteins compared to control non-BirA* (L2FC ≥1 and FDR <0.05). **(I)** 24 actinin neighborhood proteins that were exclusive to the Z-disk stage assembly were analyzed by GO and enrichment terms are listed (L2FC ≥1 and FDR <0.05 in cTnT-WT relative to control non-BirA*).

(J) 47 proteins enriched with cTnT-dependent sarcomere assembly were analyzed by GO and enrichment terms are listed (L2FC ≥1 and FDR <0.05 in cTnT-WT relative to cTnT-KO).

(K) -Log₁₀FDR (y-axis) plotted against the L2FC of cTnT-WT samples relative to cTnT-KO (x-axis) using the 294 Actinin-BirA*-enriched proteins, which identified 47 proteins (pink) that are further enriched with cTnT-dependent sarcomere assembly (L2FC ≥1 and FDR <0.05).

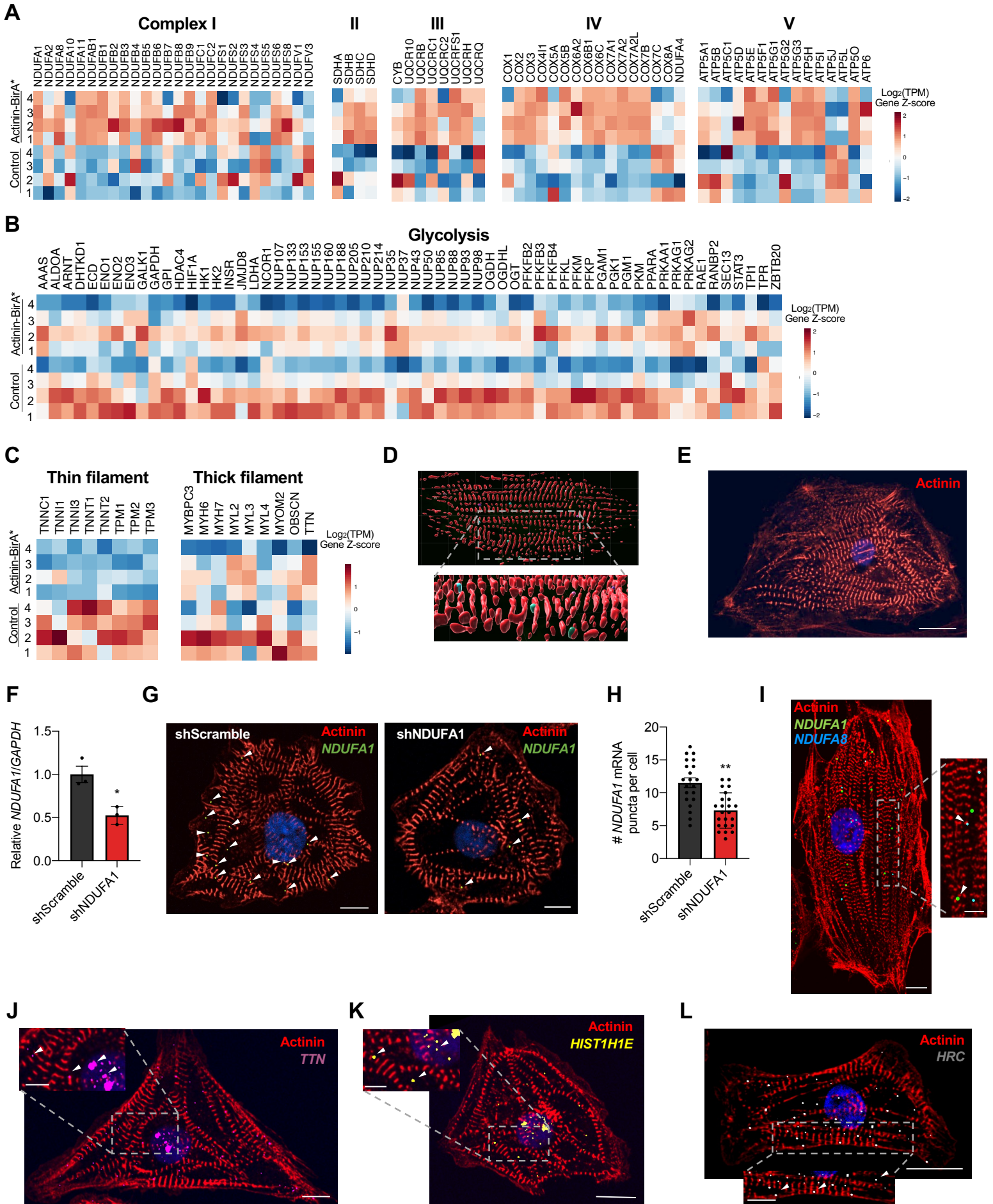
Figure S2

Figure S2. Identification of transcripts bound to RNA-binding proteins in actinin neighborhoods. (Related to Figure 2)

(A) Heatmap displaying relative expression of ETC Complexes (I-V) genes in control non-BirA* and Actinin-BirA* RIP-seq samples.

(B) Heatmap displaying relative expression of glycolysis genes in control non-BirA* vs. Actinin-BirA* RIP-seq samples.

(C) Heatmap displaying relative expression of sarcomere thin and thick filament genes in control non-BirA* vs. Actinin-BirA* RIP-seq samples.

(D) Representative image from Imaris utilizing distance transformation tool to determine distance between actinin puncta (red) and mRNA puncta (multi-colored).

(E) Representative control confocal micrograph of iPSC-CMs decorated with antibodies to actinin (red) and DAPI DNA co-stain (blue) without RNA FISH probe (scale bar=10 μ m).

(F) qPCR analysis of transcript levels of *NDUFA1* after *NDUFA1* knockdown.

(G) Representative confocal micrographs of iPSC-CMs transduced with either shScramble or shNDUFA1 and decorated with antibodies to actinin (red), DAPI DNA co-stain (blue), and RNA FISH probes against *NDUFA1* (green) (scale bar=10 μ m).

(H) Quantification of *NDUFA1* mRNA puncta per cell comparing iPSC-CMs transduced with either shScramble or shNDUFA1 (n=20).

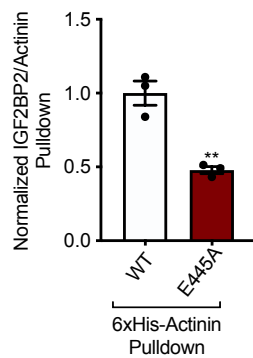
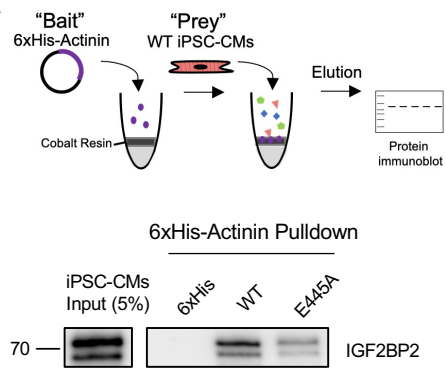
(I) RNA FISH of ETC Complex I components *NDUFA1* and *NDUFA8* that are both in proximity to actinin but not overlapped (scale bars: main image=10 μ m; inset=5 μ m).

(J) Representative confocal micrograph of iPSC-CMs decorated with antibodies to actinin (red), DAPI DNA co-stain (blue), and RNA FISH probe against *TTN* (purple) (scale bars: main image=10 μ m; inset=5 μ m).

(K) Representative confocal micrograph of iPSC-CMs decorated with antibodies to actinin (red), DAPI DNA co-stain (blue), and RNA FISH probe against *HIST1H1E* (yellow) (scale bars: main image=10 μ m; inset=5 μ m).

(L) Representative confocal micrograph of iPSC-CMs decorated with antibodies to actinin (red), DAPI DNA co-stain (blue), and RNA FISH probe against *HRC* (gray) (scale bars: main image=10 μ m; inset=5 μ m).

Data are n \geq 3; mean \pm SEM; significance assessed by Student's t-test (F, H) and defined by $P < 0.05$ (*), $P \leq 0.01$ (**).

Figure S3**A****B**

RNA Binding Protein	Method			
	TMT	SP-IP	HA-IP	M2H
IGF2BP2	+	+	+	+
PCBP1	+	+	+	-
PCBP2	+	+	+	-
SERBP1	+	+	-	-

Figure S3. Fine mapping actinin interactions with the RNA-binding protein IGF2BP2. (Related to Figure 3)

A) Purified recombinant 6xHis, 6xHis-Actinin-WT, and 6xHis-Actinin-E445A were incubated with iPSC-CM lysate in resin (diagram), and precipitates were analyzed (left) and quantified (right) by immunoblotting with anti-Actinin antibody. Equal amounts of each recombinant protein were loaded onto resin.

B) Summary overview of RBP and actinin interaction data.

Data are n=3; mean \pm SEM; significance assessed by Student's t-test (A) and defined by $P \leq 0.01$ (**).

Figure S4

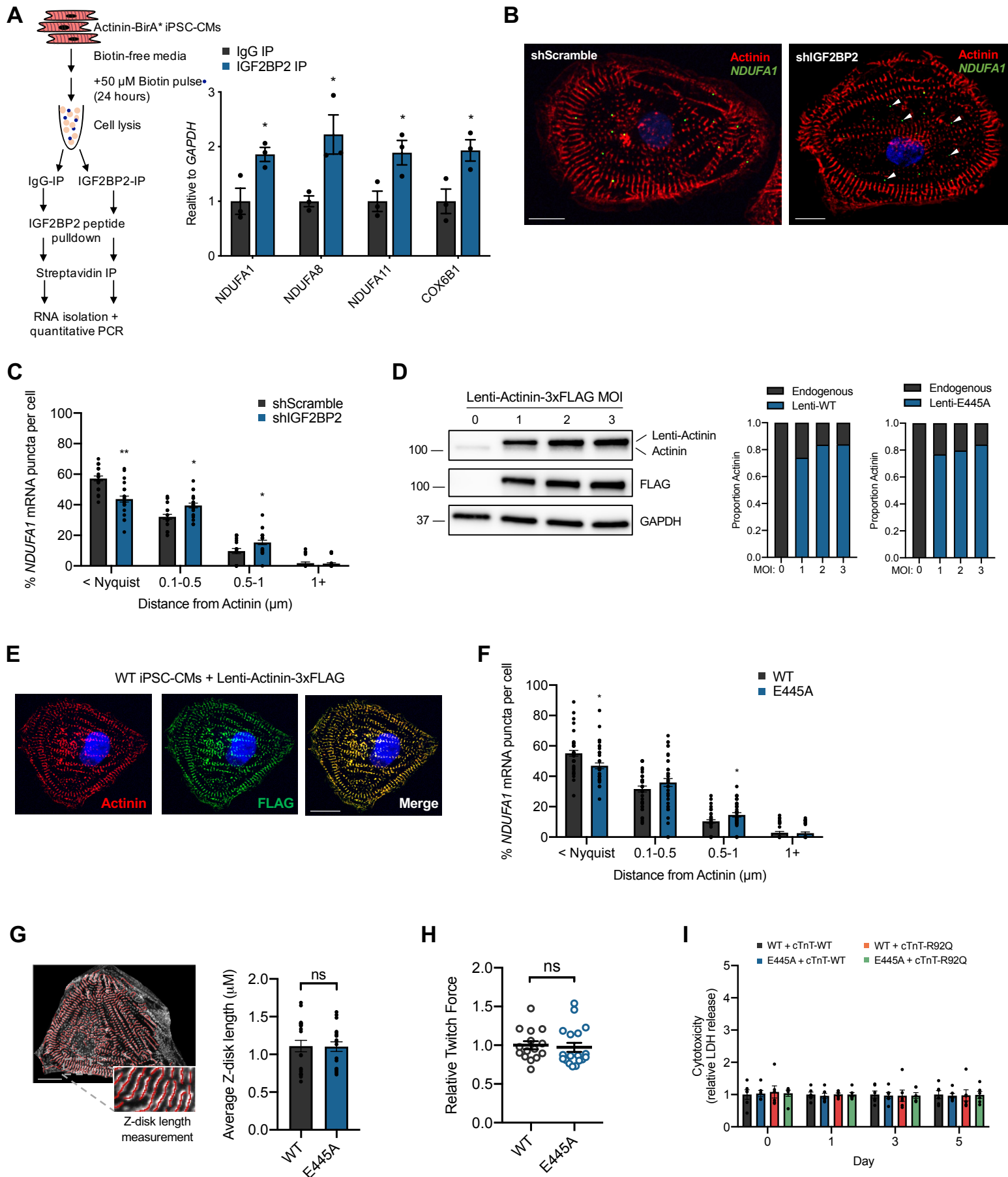


Figure S4. Actinin-IGF2BP2 interactions regulate ETC transcript localization to actinin neighborhoods and metabolic adaptation to hypercontractility in an HCM model. (Related to Figure 4)

(A) Overview of tandem-IP process (left) and qPCR results of IgG vs. IGF2BP2 IP (right) for candidate ETC transcripts.

(B) Representative confocal micrographs of iPSC-CMs transduced with shScramble or shIGF2BP2 and decorated with antibodies to actinin (red), DAPI DNA co-stain (blue), and RNA FISH probes against *NDUFA1* (green) (scale bar=10 μ m).

(C) Quantification of *NDUFA1* RNA proximity to actinin protein in iPSC-CMs treated with shScramble or shIGF2BP2 (n=25 cells).

(D) Representative immunoblots (left) and quantification (right) of MOI testing for lenti-Actinin-3x-FLAG to assess proportion of endogenous and overexpressed actinin levels.

(E) Representative confocal micrograph of iPSC-CMs decorated with antibodies to actinin (red), FLAG (green), and DAPI DNA co-stain (blue) showing appropriate localization of overexpression lenti-Actinin-3x-FLAG (scale bar=10 μ m).

(F) Quantification of *NDUFA1* RNA proximity to actinin protein in iPSC-CMs treated with overexpression of lenti-Actinin-WT or lenti-Actinin-E445A (n=40 cells).

(G) Quantification of Z-disk length by actinin stain of iPSC-CMs overexpressing lenti-Actinin-WT or lenti-Actinin-E445A (n=20) (scale bar=10 μ m).

(H) Cardiac microtissues with overexpression of lenti-Actinin-WT vs. lenti-Actinin-E445A have similar twitch force compared to controls (n=15-18).

(I) LDH activity of media supernatant collected from iPSC-CMs expressing either lenti-Actinin-WT or lenti-Actinin-E445A with lenti-cTnT-WT or lenti-cTnT-R92Q in glucose-rich media for 5 days.

Data are n \geq 3; mean \pm SEM; significance assessed by Student's t-test (A, C, F-H) or by ANOVA using Holm-Sidak correction for multiple comparisons (I) and defined by $P > 0.05$ (ns), $P < 0.05$ (*), $P \leq 0.01$ (**).